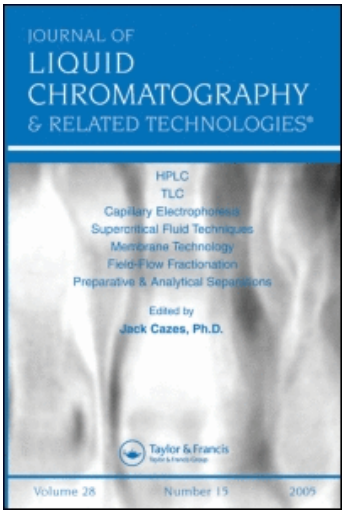

Journal of Liquid Chromatography & Related Technologies

Publication details, including instructions for authors and subscription information:
http://www.informaworld.com/smpp/title~content=t713597273

Cylindrical Splitt and Quadrupole Magnetic Field in Application to Continuous-Flow Magnetic Cell Sorting

M. Zborowski[a]; P. S. Williams[b]; L. Sun[c]; L. R. Moore[a]; J. J. Chalmers[c]

[a] Department of Biomedical Engineering, The Cleveland Clinic Foundation 9500 Euclid Avenue, Cleveland, OH, USA [b] Field-Flow Fractionation Research Center University of Utah, Salt Lake City, UT, USA [c] Department of Chemical Engineering, The Ohio State University, Columbus, OH, USA

To cite this Article Zborowski, M. , Williams, P. S. , Sun, L. , Moore, L. R. and Chalmers, J. J.(1997) 'Cylindrical Splitt and Quadrupole Magnetic Field in Application to Continuous-Flow Magnetic Cell Sorting', Journal of Liquid Chromatography & Related Technologies, 20: 16, 2887 — 2905

To link to this Article: DOI: 10.1080/10826079708005599

URL: http://dx.doi.org/10.1080/10826079708005599

J. LIQ. CHROM. & REL. TECHNOL., 20(16 & 17), 2887–2905 (1997)

CYLINDRICAL SPLITT AND QUADRUPOLE MAGNETIC FIELD IN APPLICATION TO CONTINUOUS-FLOW MAGNETIC CELL SORTING

M. Zborowski,[1] P. S. Williams,[2] L. Sun,[3]
L. R. Moore,[1] J. J. Chalmers[3]

[1] Department of Biomedical Engineering
The Cleveland Clinic Foundation
9500 Euclid Avenue
Cleveland, OH 44195-5254, USA

[2] Field-Flow Fractionation Research Center
University of Utah
Salt Lake City, UT 84102, USA

[3] Department of Chemical Engineering
The Ohio State University
Columbus, OH 43210-1080, USA

ABSTRACT

The quadrupole magnetic field has been used for quadrupole mass spectroscopy and for industrial and mining dry separations. We propose to use it for rapid, continuous-flow cell sorting in biomedical and biotechnological applications. We set out to investigate the performance of such a sorter using the theoretical methods of split-flow thin channel separation (SPLITT). Comparison of theoretical results and preliminary experimental

data, using a model system of human peripheral lymphocytes labeled with immunomagnetic colloid, led us to the identification of the most important parameters of the system.

INTRODUCTION

Magnetic cell separation has become an important part of research related to cell surface chemistry and cell function.[1,2] It relies on the development of antibodies against cell surface markers, and suitable magnetic labels.[3] It has been successfully applied, also, to bone marrow transplantation therapy and stem cell transplantation.[4,5] The current, state-of-the art, commercial magnetic cell separators operate on the basis of a batch process.[1,3] The advantage of the batch process is relative simplicity of the separator design and its use. The disadvantages of such a process are limitations in the separator performance, such as unequal treatment of enriched and depleted fractions, and limited sorting capacity.[6]

Small (molecular or colloidal) magnetic label and a well-defined and simple magnetic field geometry are prerequisites for continuous-flow cell sorting. The advantages of using submicrometer, colloidal magnetic particles for cell separation have been recently recognized.[6] High purity and high recovery separation of the positive cell fraction have been achieved using such colloidal labels and high-gradient magnetic separation (HGMS).[1,6] The small size, and small magnetization, of the microbead require higher fields and gradients than the particulate label. However, the small size of the beads offers better control over cell motion in the aqueous solution than is possible with the use of large, particulate bead.

We identified the quadrupole magnetic field as a field of particular simplicity and, therefore, promising for a continuous-flow cell separation.[7] In designing the quadrupole field separator with its characteristic annular flow of separands and carrier medium, and the presence of flow split cylinders at the inlet and outlet ports, we noted analogies with the SPLITT technique.[8-11] These observations lead us to the conclusion that the further development of magnetic cell sorting could be accelerated by combining existing theoretical and experimental methods of SPLITT with the theory of the quadrupole magnetic field. The aim of this study is the preliminary investigation of analogies between the processes of quadrupole magnet sorting and SPLITT. In particular, we set out to predict the resolution, purity, recovery, and throughput of the sorted fractions using the mathematical formalism developed for SPLITT separation, and compare these with the preliminary experimental data.

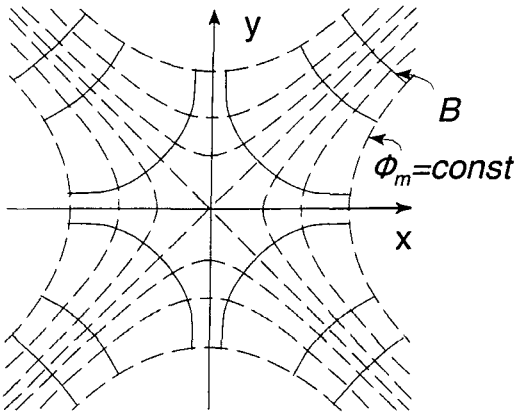

Figure 1. Equipotential, ϕ_m = const., and field, B, lines of the quadrupole field.

MATERIALS AND METHODS

Theory

The collective effect of the external magnetic field, $\boldsymbol{H}$, on the colloidal magnetic labels bound to the cell surface leads to the linear relationship between cell magnetic moment, μ, and $\boldsymbol{H}$, $\mu = V\chi\boldsymbol{H}$. In a diamagnetic medium (such as water) $\boldsymbol{B} = \mu_0\boldsymbol{H}$ [T], where $\boldsymbol{H}$ [A/m] is magnetic field strength.[12] The magnetostatic force, $\boldsymbol{F}_m$, acting on the labeled cell, is given by the expression (in SI system of units):

$$F_m = (\mu \cdot \nabla)B = V\chi(H \cdot \nabla)B = 1/2\frac{V_{cell}\,\Delta\chi}{\mu_0}\nabla B^2 \qquad (1)$$

where χ - the volumetric magnetic susceptibility [dimensionless], $\Delta\chi$ - the difference between the volume-averaged magnetic susceptibility of the cell and that of the medium, V_{cell} - cell volume [m^3], and $\mu_0 = 4 \times 10^{-7}$ [Tm/A]. Note that the magnetostatic force acting on a freely suspended dipole follows the lines of the steepest increase of B^2. In homogenous media, such as aqueous solutions of electrolytes, the value of B^2 is directly proportional to the magnetic field energy density. The properties of the small magnetic particles in the external magnetostatic field are such that one is justified in using the scalar potential field, ϕ_m, to describe their motion, where $\boldsymbol{H} = -\nabla\phi_m$.

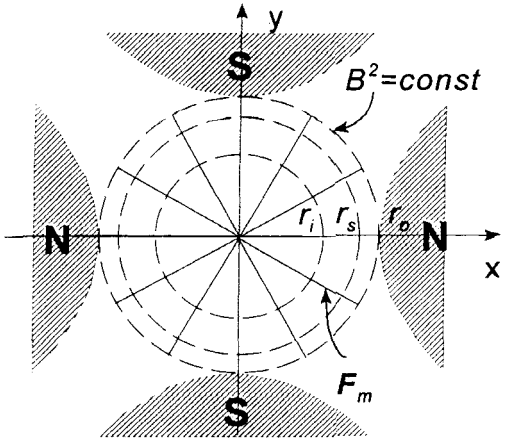

Figure 2. Constant field energy density, B^2 = const., and force, F_m, lines acting on a freely-suspended magnetic dipoles in the quadrupole field. The magnetic particles migrate radially between r_i - inner cylinder radius, through r_s - split cylinder radius, towards r_o - outer cylinder radius.

The quadrupole field is defined by the linear dependence of $\boldsymbol{B}$ on the radial coordinate.[7] The equipotential, ϕ_m = const., and field, B, lines of the quadrupole field are shown in Fig. 1. The magnetic force acting on the magnetic dipole in the quadrupole field is obtained from the definition of the quadrupole field, and from the relation in Eq. 1:

$$B = B_0 r' \qquad (2)$$

$$F_m = \frac{V_{cell}}{\mu_0}\frac{\Delta\chi}{r_0}\frac{B_0^2}{r_0} r', \quad \phi \in [0,2\pi]$$

where (r, ϕ) are cylindrical coordinates, r_0 is the aperture radius at the pole tips, $\boldsymbol{r}' = \boldsymbol{r}/r_0$, and B_0 is the magnetic field at the pole tip, $B_0 = B(\mathbf{r})$, Fig. 2.

The order of magnitude of F_m can be calculated using the following parameters, characteristic of a practical system: B_0 = 0.5 T, $r_0 = 5{+}10^{-3}$ m, $V_{cell} = 4/3\pi(5\ \mu m)^3 = 524\ \mu m^3 = 5{+}10^{-16}$ m^3, $\Delta\chi = 100\ 10^{-6}$ (in SI system of units). Assuming $r' = 1$, O[F_m] = 10^{-12} N, which is well within the resolving power of SPLITT.[13]

Geometrical Similarity Between Quadrupole Field Separator and SPLITT

The radial migration of magnetically-labeled cells in the quadrupole field, along the force lines defined by Eq. 2, dictates the separator geometry. The preferred geometry is that of a thin annulus pressed against the pole tips of the quadrupole magnet, with the cylindrical flow splitters inserted at inlet and outlet ends of the annulus. The cell mixture is injected into the portion of the flow contained between the split cylinder and the inside cylinder, as shown in Fig. 2, which also represents the plan view (cross-section) of the separator. The separation is achieved by the differential radial migration of cells – the magnetically-labeled cells migrate in the outward direction, Eq. 2, while the unlabeled cells remain in the vicinity of the inside cylinder wall. Given sufficient time (or length of the separation channel), the magnetic cells are sufficiently displaced towards the outer cylindrical wall of the annulus so that they can be collected between the outlet flow splitter and the outer cylindrical wall, Fig. 3. The unlabeled cells follow the flow streamlines and are collected between the inside cylindrical wall and the flow splitter.

The elevation view of the quadrupole field separator, Fig. 3, reveals characteristic features of a SPLITT separator, i.e., split flows at the inlet and outlet portions of the channel, labeled a', b', and a, b, respectively, and the thin flow channel exposed to the separation force (magnetic) normal to the general direction of flow.[8-11] It may be noted that the magnetic force is independent of angular coordinate, and is directly proportional to radial coordinate, Eq.2.

The important distinguishing feature of the quadrupole field separator is its axial symmetry, unlike any of the SPLITT channels described to date, which are all rectangular. Retention by field-flow fractionation in annular channels has been described before.[14] This formal analogy between the quadrupole field separator and SPLITT is the basis of mathematical analysis of the separator performance presented below.

Cell Trajectory Within the Quadrupole Field SPLITT System

Radial position of splitting cylinders

The splitting cylinders are equivalent to the splitting planes of conventional SPLITT systems. The inlet splitting cylinder (ISC) lies between the streamlines originating at the two different inlets, and the outlet splitting cylinder (OSC) lies between the streamlines exiting the different outlets, Fig. 3.

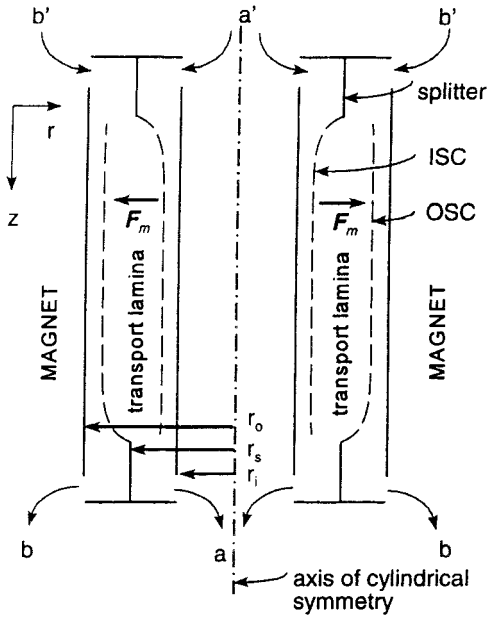

Figure 3. Elevation view of the cylindrical SPLITT quadrupole magnetic field sorter. ISC - inlet splitting cylinder, OSC - outlet splitting cylinder. Cell sample is fed through port *a'*, carrier medium is pumped through port *b'*, sorted fractions are collected at ports *a* and *b*.

The velocity profile within the annulus[15] is given by the equation

$$v(r') = \frac{2 < v >}{A_1}(1 - r'^2 - A_2 \ln r') \qquad (3)$$

where $r' = r/r_0$, $r'_i < r' \leq 1$, r'_i corresponds to the radius of the inner cylinder, $A_2 = (1-r'^2_i)/\ln r'_i$, $A_1 = 1 + r'^2_i + A_2$,and $<v>$ is the mean fluid velocity. The total volumetric flowrate $\dot{V}$ is given by

$$\dot{V} = \pi r_0^2 (1 - r_i'^2) < v > \qquad (4)$$

while the volumetric flowrate $\dot{V}_a$ between the inner wall and some radial position r_a is given by

$$\dot{V}_a = \int_{r_i}^{r_a} 2\pi r v(r) dr = \frac{4\pi r_0^2 < v >}{A_1} \int_{r'_i}^{r'_a} r'(1 - r'^2 - A_2 \ln r') dr' \quad (5)$$

Hence

$$\frac{\dot{V}_a}{\dot{V}} = \frac{2r'^2_a - r'^4_a - 2A_1 r'^2_a \ln r'_a + A_1 r'^2_a - r'^4_i - A_1 r'^2_i}{(1 - r'^2_i)(1 + r'^2_i + A_1)} \quad (6)$$

Cell trajectory within the system

Radial velocity at position r' is given by

$$u(r') = \frac{F_m}{6\pi\eta R} = \frac{2R^2 \Delta\chi}{9\eta\mu_0} \frac{B_0^2}{r_0} r' \quad (7)$$

where η is the fluid viscosity and R is cell radius. We can write $u(r')$ as $r_0 dr'/dt$, and $v(r')$ as dz/dt, and it follows that $dz = (r_0 v(r')/u(r'))dr'$. Hence,

$$\int_0^L dz = \int_{r'_1}^{r'_2} \frac{2 < v > r_0}{A_1} (1 - r'^2 - A_2 \ln r') \frac{9\eta\mu_0}{2R^2 \Delta\chi} \frac{r_0}{B_0^2} \frac{dr'}{r'} \quad (8)$$

where r'_1 and r'_2 correspond to the initial and final radial positions of a cell passing through the system. On integrating and rearranging, we obtain the result

$$\Delta\chi = \frac{9\dot{V}\eta\mu_0}{\pi A_1 L R^2 B_0^2 (1 - r'^2_i)} \left[\ln r' - \frac{r'^2}{2} - \frac{A_2}{2} (\ln r')^2 \right]_{r'_1}^{r'_2} \quad (9)$$

which we can write as $\Delta\chi = K_s \dot{V} I(r'_1, r'_2)$ in which K_s depends on fixed system parameters and dimensions and is given by

$$K_s = \frac{9\eta\mu_0}{\pi A_1 L R^2 B_0^2 (1 - r'^2_i)} \quad (10)$$

and

$$I(r'_1, r'_2) = \left[\ln r' - \frac{r'^2}{2} - \frac{A_2}{2}(\ln r')^2 \right]_{r'_1}^{r'_2} \qquad (11)$$

Let F_b denote the ratio of the number of the magnetically-labeled cells exiting the outlet port b to that entering the inlet port a'. It follows that if r'_{ISC} and r'_{OSC} represent the radial positions of the inlet and outlet splitting cylinders, respectively, then

$$F_b = 0 \text{ if } \Delta\chi \leq K_s \dot{V} I(r'_{ISC}, r'_{OSC}) \qquad F_b = 1 \text{ if } \Delta\chi > K_s \dot{V} I(r'_i, r'_{OSC}) \qquad (12a,b)$$

If we assume that a cell is damaged and/or does not exit the system if it contacts the outer wall, then we also have

$$F_b = 1 \text{ if } \Delta\chi < K_s \dot{V} I(r'_{ISC}, 1) \qquad F_b = 0 \text{ if } \Delta\chi \geq K_s \dot{V} I(r'_i, 1) \qquad (13a,b)$$

It is possible for $F_b = 1$ only if conditions (12b) and (13a) are fulfilled. Then suppose we require $F_b = 1$ for some range of $\Delta\chi$ from $\Delta\chi_{low}$ to $\Delta\chi_{high}$; it is apparent that flow conditions must be set up such that

$$\Delta\chi_{low} = K_s \dot{V} I(r'_i, r'_{osc}) \text{ and } \Delta\chi_{high} = K_s \dot{V} I(r'_{isc}, 1) \qquad (14)$$

for which we require that $I(r'_{ISC}, 1) > I(r'_i, r'_{OSC})$ and $r'_{ISC} < r'_{OSC}$.

Setup of flow regime

For the present system $r'_i = 0.5$. Consider $r'_{ISC} = 0.6$ and $r'_{OSC} = 0.75$, and suppose we require $\Delta\chi_{low}$ and $\Delta\chi_{high}$ to bracket $\Delta\chi$ of $150 \cdot 10^{-6}$, so that

$$\frac{\Delta\chi_{low} + \Delta\chi_{high}}{2} = 150 \cdot 10^{-6} \qquad (15)$$

From equations (14) we see that

$$K_s \dot{V} = \frac{\Delta\chi_{low}}{I(0.5,0.75)} = \frac{\Delta\chi_{high}}{I(0.6,1.0)} \quad (16)$$

For the present system parameters and dimensions these equations may be solved to obtain $\Delta\chi_{low} = 122 \cdot 10^{-6}$, $\Delta\chi_{high} = 178 \cdot 10^{-6}$, and $\dot{V} = 3.782$ mL/min. For the assumed r'_{ISC} and r'_{OSC} we obtain the required sample feed flowrate $\dot{V}(a') = 0.323$ mL/min, outlet flow rate adjacent to the inner wall $\dot{V}(a) = 1.710$ mL/min, and outlet flow rate adjacent to the outer wall $\dot{V}(b) = 2.072$ mL/min.

We may also calculate that $F_b = 0$ for $\Delta\chi \leq 91 \cdot 10^{-6}$ and for $\Delta\chi \geq 209 \cdot 10^{-6}$, the latter corresponding to cells that contact the outer wall before exiting the system.

EXPERIMENTAL

The test cell model system consisted of human peripheral lymphocytes, collected from healthy volunteer donors in accordance with the CCF Institutional Review Board guidelines. The mononuclear cell fraction, rich in lymphocytes (90-95%), with an admixture of monocytes (5-10%) and occasional contamination of erythrocytes, was obtained by centrifugation on a Ficoll cushion. The cells were handled using routine laboratory procedures.[16]

Lymphocytes were targeted using monoclonal antibodies (mAb) against T cytotoxic cells (bearing CD8 surface marker). The cells were labeled using a sandwich of primary antibody-fluorescein (FITC) conjugate, and secondary antibody-magnetic label (MACS) conjugate (MACS microbeads, Miltenyi Biotec, Auburn, CA). The presence of the iron dextran particle on the cell conferred on it the magnetic susceptibility $\Delta\chi$. The indirect magnetic label method was selected for its versatility and the magnetic susceptibility amplification. The use of fluorescein-conjugate sensitized the magnetically-labeled cells to UV light and made them visible to FACS analysis. The small label did not interfere with the FACS analysis, and the FACS analysis could be performed directly on the sorted cell fractions, to measure the sorter performance. A typical cell fluorescence histogram by FACS analysis is shown in Fig. 6(a) (by FACScan Analyzer, Becton-Dickinson, San Jose, CA). Each test sample was accompanied by negative controls for non-specific labeling by primary and secondary antibodies, and a positive control using a primary, but not secondary, antibody (not shown).

Table 1

Summary of CD8 Lymphocyte Sorting in Quadrupole Magnetic Field

#	Purity %[a]			Recovery %[b]						Total Cell No.	Cell Sorting Cap.
	a'	a	b	F_a	F_b	Total	$\dot{V}$[c] (mL/min)	$\frac{\dot{V}(a')}{\dot{V}}$	$\frac{\dot{V}(b')}{\dot{V}}$	x10^6	cell/s
1	27	21	54	60	11	71	3.1	0.45	0.55	6.5	12,000
2	20	16	48	49	37	86	3.1	0.41	0.59	10.1	10,000
3	25	21	52	54	27	81	3.1	0.45	0.55	12.5	12,000
4	16	9	24	26	38	64	3.1	0.1	0.88	3.4	4,800
5	22	11	31	41	30	71	3.1	0.1	0.88	7.6	6,000

[a] Purity: percent CD8 cell fraction; [b] Recovery: ratio of absolute CD8 cell count in the sorted fraction to that in feed; [c] $\dot{V} = \dot{V}(a') + \dot{V}(b') = \dot{V}(a) + \dot{V}(b)$ total flow rate.

The quadrupole field was generated by permanent magnets (28 MGOe cobalt-iron-boron magnets from Dexter Magnetics, Toledo, OH). Maximum field, $B_0 = 0.5$ T, gradient, $\partial B/\partial r = 0.1$ T/mm. Magnet aperture was 9.53 mm, length 64.5 mm. The inner cylinder diameter was $2r_i = 4.76$ mm, split cylinder inner diameter was $2r_s = 6.44$ mm, thickness 0.35 mm. The flow rate was controlled by syringe pumps (Harvard Apparatus, Natick, MA) connected by 0.8 mm i.d. Teflon® tubing to ports *a'*, *b'*, and *b* (port *a* was left open to atmosphere to equilibrate the pressure). The volumetric flow rates were varied as indicated in Table 1. The following parameters were calculated to describe the quadrupole field sorter performance: (1) purity - percent CD8 fluorescent cell subpopulation in each fraction (as measured by flow cytometry); (2) recovery or retrieval factor, F_b - ratio of absolute CD8 cell count in the sorted fraction to that in feed; (3) sorting capacity: total number of cells sorted in a given time interval.

RESULTS

Trajectory simulations were performed for ten initial cell positions set equidistant between the inner wall, r_i, and the inlet splitting cylinder, r_{ISC}, Fig. 4. The cells migrated radially, across the annular transport lamina defined by the radii r_{ISC} and r_{OSC}. The following extreme cases are illustrated in Figs. 4(a),

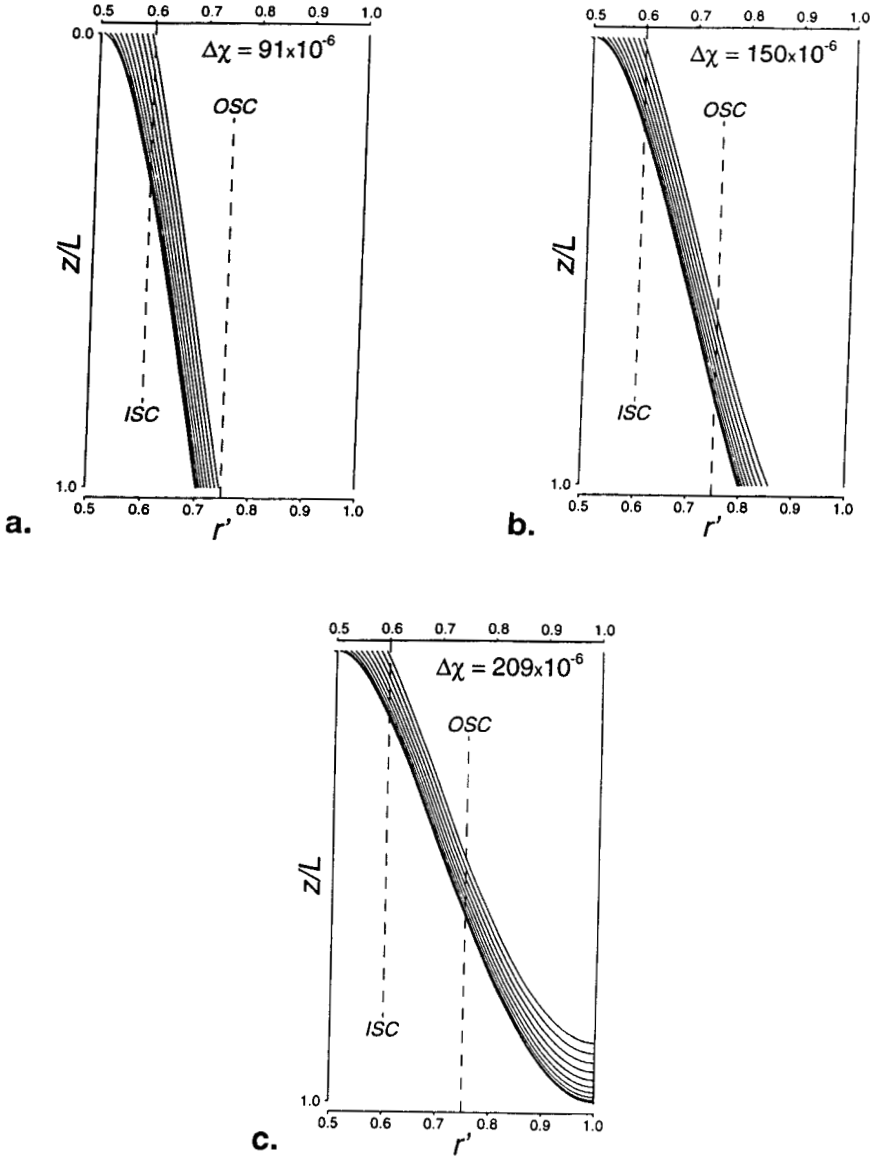

Figure 4. Examples of magnetically-labeled cell trajectories in the cylindrical SPLITT channel. The net average cell magnetic susceptibilities, $\Delta\chi$, are indicated; $r' = r/r_o$.

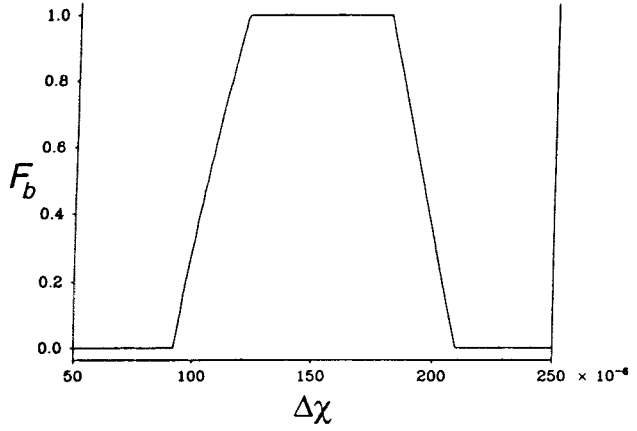

Figure 5. Fractional recovery, F_b, of the magnetically-labeled cells at the port *b*, as a function of net average cell magnetic susceptibility, $\Delta\chi$.

(b), and (c): depending on the value of the net cell magnetic susceptibility, $\Delta\chi$, either none of the magnetically-labeled (positive) cells traversed the transport lamina during the residence time in the magnetic field and, therefore, were re-collected at the *a*-port ($F_b = 0$, see Fig. 4(a)); or all of the positive cells crossed the transport lamina, without hitting the outer wall, and were collected in the *b*-port ($F_b = 1$, Fig. 4(b)); or all of the positive cells hit the outer wall and therefore were lost to the separation ($F_b = 0$, Fig. 4(c)).

The results of trajectory simulations are summarized in Fig. 5. One must bear in mind that the numerical values shown in Figs. 4 and 5 depend on the selected flowrates $\dot{V}$, $\dot{V}(a')$, $\dot{V}(b)$, and that the results shown in these figures were selected for the purpose of illustrating the characteristic features of the separator, rather than presenting any particular result. One may interpret the results shown in Fig. 5 considering two different cell model systems: 1) consisting of a group of different sets of cells, $i = 1, \ldots N$, each characterized by a discrete value of cell magnetic susceptibility, $\Delta\chi_i$; and 2) consisting of a single set of cells characterized by a continuous distribution of $\Delta\chi$ among cells in the set. The prediction of cell separation results differs depending on which cell model system one uses to approximate the actual situation. According to model number one, one may hope to obtain a complete recovery of all positive cells in the *b*-port (and thus a complete separation) if one matches the cell set $\Delta\chi_i$ with the range of $\Delta\chi$ for which $F_b = 1$ in the separator (such as $91\ \ 10^{-6} \leq \Delta\chi < 209\ \ 10^{-6}$; see Fig. 5). In short, model one predicts a possibility of an all-or-

nothing outcome of the separation. According to model number two, one may never hope to obtain a complete separation of positive from negative cells because there will be always positive cells in the sample such that $\Delta\chi < 91+10^{-6}$ or $\Delta\chi \geq 209+10^{-6}$, Fig. 5. The actual value of the fractional cell recovery in the *b*-port will depend on how many cells fall outside of the range between the low and high value of $\Delta\chi$, or, in other words, on the dispersion of the $\Delta\chi$ distribution in the cell sample.

The preliminary experiments establishing the feasibility of the cell separation method were performed using human lymphocytes tagged with immunofluorescent label and magnetic colloid, Fig. 6. In five experiments, the cell sample of 16% to 27% CD8 cell purity was fed into the *a'*-port, the cell medium was fed into the *b'*-port, and the sorted fractions were collected at *a*- and *b*-ports; see Fig. 3. The changes in cell sample fluorescence histograms following magnetic sorting indicated an increase of CD8 cell purity in the *b*-port, and therefore enrichment of positive (fluorescent) cells, up to 54% of CD8 cell purity. The recovery of the enriched cells, F_b, was rather low, 11% to 38%, and had a tendency to increase with the decreasing purity of the enriched cell fraction, Table 1. This indicates contamination of the positive fraction by negative cells due to less-than-optimal flow conditions inside the channel. The fact that the total CD8 cell recovery was less than 100% indicated cell loss due to magnetic deposition on the outside cylinder wall (and possibly elsewhere in the flow system). This, and the contamination of negative cells by positive cells in the *a*-port, Table 1, indicated a substantial dispersion of the cell $\Delta\chi$ value and, therefore, supported the validity of the model two discussed above.

DISCUSSION

In this study, we present tentative results of continuous-flow magnetic cell sorting using the quadrupole field separator, and preliminary sorter evaluation based on analogy with the SPLITT process. The properties of the electric and magnetic quadrupole fields are well understood in applications to ionic and molecular beams.[7] The magnetic quadrupole field has been evaluated for high throughput dry separation of pulverized coal to separate the ash and pyritic fractions (weakly paramagnetic) from maceral fractions (diamagnetic).[17,18] The quadrupole magnetic field has been used to increase the efficiency of batch-type magnetic cell separation.[19] We propose that the true advantages of using the quadrupole field in cell separation are in its use for continuous-flow separation. Unlike the current high-gradient magnetic separation (HGMS) columns, the open gradient quadrupole field offers advantages of the unhindered cell flow through the high field, B, and gradient, ∇B, area, and, thus, a precise control of

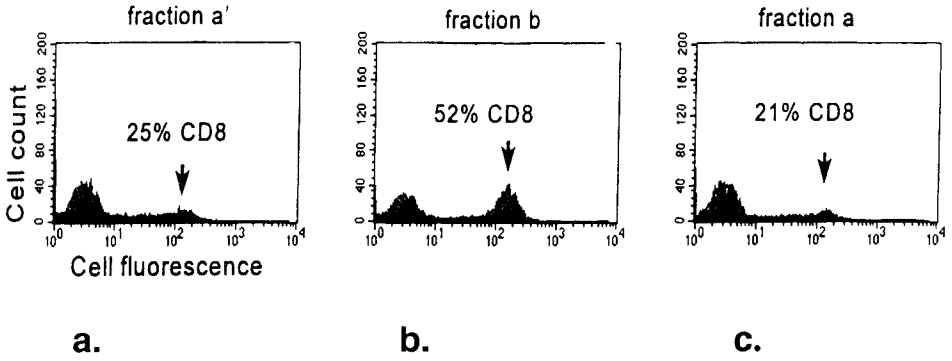

Figure 6. Experimental results of sorting of cytotoxic T cell (CD8 cells) from a mixture of human peripheral blood mononuclear cells. Note increase in purity of the magnetically-labeled CD8 cells in the *b* fraction, and a decrease of such cells in the *a* fraction. The much smaller decrease in purity in *a* fraction as compared to the increase in purity in *b* fraction is the result of a rather low recovery of these cells at the *b* - port (Table 1).

the cell trajectory. The magnetic energy gradient of the open-gradient field, ∇B^2, determining the magnetic force acting on the magnetic particle, is not limited by the magnetic properties of the components, as is the case with the high-gradient magnetic matrices, but only by the magnetomotive potential of the source. Fields of 1.6 Tesla (T), and gradients of 50 T/m were achieved in a volume of 4,000 mL in a superconducting quadrupole magnet used for the coal cleaning.[18]

Significantly, the highest separation resolution (of materials differing only slightly in the magnetic susceptibility) has been achieved in dynamic (particle stream) rather than static (batch) devices.[20] Part of the reason for this is that in the dynamic system the particles are exposed not only to the magnetic force but also to other forces (such as buoyancy and hydrodynamic drag) which contribute to the differentiation of the particles. This observation led us to a hypothesis that, in analogy to the industrial magnetic sorting in a stream, the sensitivity and specificity of the magnetic cell sorting could be increased if applied in combination with the flow, bringing it into the realm of field-flow fractionation. Deflection of the magnetically-tagged cells in a flowing stream, and separation of magnetic from non-magnetic cell fraction in a flow rather than on solid walls, requires precise information about the magnetic field geometry and flow effects on separation. Such information was provided by applying SPLITT methods to the analysis of the sorting process in the quadrupole field.

The results of this study represent work in progress and, therefore, are only a preliminary indication of the capabilities of the quadrupole field to continuous-flow cell sorting. The analysis of the system using a SPLITT analogy indicates the importance of cell susceptibility, $\Delta\chi$, distribution in the cell sample as a sorting parameter.

At the time of this study, no information about the cell $\Delta\chi$ distribution was available to us, and the experimental parameters were chosen by trial and error. This has resulted in sub-optimal selection of flow parameters, and a subsequent significant loss of high $\Delta\chi$ and low $\Delta\chi$ cell fractions, presumably due to deposition on the outer wall, and due to significant mixing with the unlabeled cells, respectively. The analogy with the SPLITT process, and the information of $\Delta\chi$ distribution for a given cell system, should provide sufficient information for selection of the best flow parameters in the future.

The current work is directed toward further study of the quadrupole cell sorting system using SPLITT formalism.

ACKNOWLEDGMENTS

This work is supported by grants NCI R01 CA62349 (M.Z.) and Whitaker Foundation (J. J. C.).

SYMBOLS AND OPERATOR DEFINITIONS

The magnitude of electromagnetic quantities were given in SI system of units (Système Internationale d'Unités).

Symbols

a, b	related to inner and outer annulus of separator outlet, respectively, (Fig. 3)
a', b'	related to inner and outer annulus of separator inlet, respectively, (Fig.3)
A	ampere, unit of electric current
A_1, A_2	constants defined below Eq. 3
$\boldsymbol{B}$	magnetic induction (magnetic flux density). In aqueous media, $\boldsymbol{B} = \mu_0\boldsymbol{H}$
B_0	magnitude of the magnetic field at the pole tips

F_a, F_b fractional recovery rates in inner and outer outlet annuli, respectively, (below Eq. 11)
$\boldsymbol{H}$ magnetic field strength
I function defined by Eq. 11
ISC Inner Splitting Cylinder, Fig.3
K_s function defined by Eq.10
m meter, unit of length
OSC Outer Splitting Cylinder, Fig.3
r_0 quadrupole magnet aperture radius; radial position of the pole tips
r_i inner cylinder radius
r_s split cylinder radius
r_{ISC}, r_{OSC} ISC and OSC radii, respectively
$r' = r/r_0$ dimensionless radial position
$\boldsymbol{r} = [x, y]$ radial coordinate
T tesla, *SI* unit of magnetic induction; corresponds to 10^4 Gauss in *em cgs* units
u radial flow linear velocity
v axial flow linear velocity
$\langle v \rangle$ spatial average of v
V volume
$\dot{V} = \dot{V}(a') + \dot{V}(b') = \dot{V}(a) + \dot{V}(b)$ total volumetric flowrate
$\dot{V}(a') = \dot{V}_{a'}$, $\dot{V}(b') = \dot{V}_{b'}$ volumetric flow rates at inner and outer inlet annuli, respectively
$\dot{V}(a) = \dot{V}_a$, $\dot{V}(b) = \dot{V}_b$ volumetric flow rates at inner and outer outlet annuli, respectively
z axial coordinate
$\mu_0 = 4 \cdot 10^{-7}$ Tm/A magnetic permeability of free space (a constant)
μ magnetic dipole moment. For a sphere of a homogenous, magnetically-polarizable medium, $\mu = V\chi\boldsymbol{H}$
ϕ angular coordinate
ϕ_m magnetic scalar potential; $\boldsymbol{H} = -\nabla\phi_m$
χ magnetic susceptibility, for homogenous media defined by the relationship between μ/V and $\boldsymbol{H}$ above
$\Delta\chi = \chi_{cell} - \chi_{medium}$ magnetic susceptibility of the cell relative to that of the medium

Vector and Operator Notation[12]

Vectors are indicated as such by the use of bold face ($\boldsymbol{A}$), their magnitude by the Roman letters (A). The Cartesian coordinates are denoted x, y, z, their

direction by unit vectors i, j, k

Scalar Product

$$A \cdot B = A_x B_x + A_y B_y + A_z B_z$$

Del or Nabla Operator

$$\nabla \equiv i\frac{\partial}{\partial x} + j\frac{\partial}{\partial y} + k\frac{\partial}{\partial z}$$

Gradient

$$\nabla \phi_m \equiv i\frac{\partial \phi_m}{\partial x} + j\frac{\partial \phi_m}{\partial y} + k\frac{\partial \phi_m}{\partial z}$$

Differentiation with respect to vector H

$$(H \cdot \nabla)A = i(H_x\frac{\partial A_x}{\partial x} + H_y\frac{\partial A_x}{\partial y} + H_z\frac{\partial A_x}{\partial z})$$

$$+ j(H_x\frac{\partial A_y}{\partial x} + H_y\frac{\partial A_y}{\partial y} + H_z\frac{\partial A_y}{\partial z})$$

$$+ k(H_x\frac{\partial A_z}{\partial x} + H_y\frac{\partial A_z}{\partial y} + H_z\frac{\partial A_z}{\partial z})$$

REFERENCES

1. A. Radbruch, B. Mechtold, A. Thiel, S. Miltenyi, E. Pflüger, Methods in Cell Biology, **42**, 387-403 (1994).

2. T. E. Thomas, P. M. Lansdorp, "Selective Separation of Cells Using Magnetic Colloids," in **Proceedings of the Fourth International Symposium on Bone Marrow Purging and Processing**, A. P. Gee, S. Gross, D. A. Worthington-White, eds., Wiley-Liss, New York, 1994, pp.65-77.

3. J. Ugelstad, P. Stenstad, L. Kilaas, W. S. Prestvik, R. Herje, A. Berge, E. Hornes, Blood Purif., **11**, 347-369 (1993).

4. A. P. Gee, Immunomethods, **5**, 232-242 (1994).

5. S. Roath, T. E. Thomas, J. H. P. Watson, P. M. Lansdorp, R. J. S. Smith, A, J. Richards, "Specific Capture of Targeted Hematopoietic Cells by High Gradient Magnetic Separation by the Use of Ordered Wire Array Filters and Tetrameric Antibody Complexes Linked to a Dextran Iron Particle," in **Proceedings of the Fourth International Symposium on Bone Marrow Purging and Processing**, A. P. Gee, S. Gross, D. A. Worthington-White, eds., Wiley-Liss, New York, 1994, pp.155-163.

6. J. T. Kemshead, "The Immunomagnetic Manipulation of Bone Marrow," in **Bone Marrow Processing and Purging. A Practical Guide**, A. P. Gee, ed., CRC Press, Boca Raton, 1991, pp. 293-305.

7. P. H. Dawson, **Quadrupole Mass Spectrometry and Its Applications**, Elsevier Scientific Publishing Company, New York, 1976.

8. J. C. Giddings, Sepn. Sci. Technol., **23**, 931-943 (1988).

9. S. Levin, J. C. Giddings, J. Chem. Tech. Biotechnol, **50**, 43-56 (1991).

10. P. S. Williams, Sepn. Sci. Technol., **29**, 11-45 (1994).

11. C. B. Fuh, E. M. Trujillo, J. C. Giddings, Sepn. Sci. Technol., **30**, 3861-3876 (1995).

12. R. Becker, **Electromagnetic Fields and Interactions**, Dover Publications Inc., New York, 1982, p.112.

13. J. C. Giddings, Science, **260**, 1456-1465 (1993).

14. J. M. Davis, J. C. Giddings, J. Phys. Chem., **89**, 3398-3405 (1985).

15. R. B. Bird, W. E. Stewart, E. N. Lightfoot, **Transport Phenomena**, John Wiley & Sons, New York, 1960, p.53.

16. G. G. B. Klaus, **Lymphocytes. A Practical Approach**, IRL Press, Oxford, 1987.

17. R. D. Doctor, C. B. Panchal, C. E. Swietlik, "Recent Advances in Separation Techniques - III," AIChE Symposium Series, **82**, 154-168 (1986).

18. R. D. Doctor, C. D. Livengood, Proceedings of the Intersociety Energy Conversion Engineering Conference, **Session 25.2**, 160-165 (1990).

19. P. A. Liberti, B. P. Feeley, "Analytical- and Process-Scale Cell Separation with Bioreceptor Ferrofluids and High Gradient Magnetic Separation," in **Cell Separation Science and Technology**, D. S. Compala, P. Todd, eds., ACS Symposium Series, Vol. 464, Washington, 1991, pp.268-288.

20. D. Lewis, T. D. Wellington, IEEE Transactions in Magnetics, MAG-12, 480-485 (1976).

Received January 17, 1997
Accepted April 10, 1997
Manuscript 4442